Int J Theor Phys (2017) 56:2363–2375
DOI 10.1007/s10773-017-3390-y

Quantum Statistical Properties of the Codirectional Kerr Nonlinear Coupler in Terms of su(2) Lie Group in Interaction with a Two-level Atom

M. Sebawe Abdalla[1] · E. M. Khalil[2,3] · A. S.-F. Obada[2]

Received: 14 December 2016 / Accepted: 13 April 2017 / Published online: 18 May 2017

Abstract The problem of the codirectional Kerr coupler has been considered several times from different point of view. In the present paper we introduce the interaction between a two-level atom and the codirectional Kerr nonlinear coupler in terms of su(2) Lie algebra. Under certain conditions we have adjusted the Kerr coupler and consequently we have managed to handle the problem. The wave function is obtained by using the evolution operator where the Heisnberg equation of motion is invoked to get the constants of the motion. We note that the Kerr parameter χ as well as the quantum number j plays the role of controlling the atomic inversion behavior. Also the maximum entanglement occurs after a short period of time when $\chi = 0$. On the other hand for the entropy and the variance squeezing we observe that there is exchange between the quadrature variances. Furthermore, the variation in the quantum number j as well as in the parameter χ leads to increase or decrease in the number of fluctuations. Finally we examined the second order correlation function where classical and nonclassical phenomena are observed.

Keywords Interaction between coupled two quantum systems · Codirectional non linear coupler · Atomic inversion · Statistical properties

✉ E. M. Khalil
eiedkhalil@yahoo.com

M. Sebawe Abdalla
m.sebaweh@physics.org

[1] Mathematics Department, College of Science, King Saud University, P.O. Box 2455, Riyadh 11451, Saudi Arabia

[2] Mathematics Department, Faculty of Science, Al-Azhar University, Nasr City 11884, Cairo, Egypt

[3] Mathematics Department, Faculty of Science, Taif University, Taif City 888, Saudi Arabia

1 Introduction

It is well known that there are three important processes in nonlinear optics, namely, up-conversion, down-conversion and Kerr-like process. The optical coupler is a device composed of two (or more) waveguides, which are placed close enough to allow exchanging energy between waveguides via evanescent waves [1]. Recently, this device has attracted much attention for several reasons. The progress in the optics communication and quantum computing networks requires data transmission [2–4], and this simple device has potential applications in all-optical switching [5–7]. Furthermore, it provides electromagnetic fields with an exceptionally wide range of nonclassical effects. Most importantly this device has been implemented [8–14] and applied in many experimental approaches, e.g. in picosecond switching induced by saturable absorption [15], optical multi-mode interference devices based on self-imaging [16], and photonic bandgap structures in planar nonlinear waveguides [17]. There are different types of directional couplers [18–20]; symmetric couplers (linear or nonlinear processes are involved in both the waveguides), asymmetric coupler [21–25] (at least one of the waveguides possesses different nonlinearity than the others).

It is well known that the directional Kerr non linear coupler has attracted much attention in the field of quantum optics, as a result of its applications in optics as an intensity dependent routing switch [21, 22]. The Hamiltonian controlling the co-directional Kerr nonlinear coupler is given as [7, 26]

$$\frac{\hat{H}}{\hbar} = \sum_{i=1}^{2}\left[(\omega_i)\,\hat{a}_i^{\dagger}\hat{a}_i + \chi_i\left(\hat{a}_i^{\dagger 2}\hat{a}_i^{2}\right)\right] + \bar{\chi}\prod_{i=1}^{2}\hat{a}_i^{\dagger}\hat{a}_i + \lambda\left(\hat{a}_1^{\dagger}\hat{a}_2 + \hat{a}_2^{\dagger}\hat{a}_1\right) \tag{1}$$

where ω_1 and ω_2 are the frequencies of the first and the second modes with the annihilation operators $\hat{a}_1$ and $\hat{a}_2$, respectively, $\bar{\chi}$ and $\chi_i, i = 1, 2$ are the coupling constants proportional to the third order susceptibility $\chi^{(3)}$ and responsible for the self-action and cross-action processes, respectively, and λ is the linear coupling constant between the waveguides. Note that

$$\left[\hat{a}_i, \hat{a}_j^{\dagger}\right] = \delta_{i,j}, \qquad \delta_{i,j} = \begin{vmatrix} 1 & i = j \\ 0 & i \neq j \end{vmatrix} \tag{2}$$

Now if we define $\hat{J}_+ = \hat{a}_1^{\dagger}\hat{a}_2$, and $\hat{J}_- = \hat{a}_2^{\dagger}\hat{a}_1$, such that

$$\left[\hat{J}_+, \hat{J}_-\right] = 2\hat{J}_z, \qquad \left[\hat{J}_z, \hat{J}_\pm\right] = \pm\hat{J}\pm \tag{3}$$

with $\hat{J}_z = \frac{1}{2}\left(\hat{n}_1 - \hat{n}_2\right)$ and consider $\omega_2 = -\omega_1 = \frac{\omega}{2}$, then we cast the Hamiltonian (1) in the following form:

$$\frac{\hat{H}}{\hbar} = \omega\hat{J}_z + \chi\hat{J}_z^2 + \lambda\left(\hat{J}_- + \hat{J}_+\right) \tag{4}$$

where we have taken $\chi_1 = \chi_2 = \chi$ and $\bar{\chi} = -2\chi$. On the other hand if we inject a two-level atom within the waveguides, this would lead to change the above Hamiltonian (4) to the following one:

$$\frac{\hat{H}}{\hbar} = \omega\hat{J}_z + \frac{\omega_0}{2}\hat{\sigma}_z + \chi\hat{J}_z^2 + \lambda\left(\hat{J}_-\hat{\sigma}_+ + \hat{J}_+\hat{\sigma}_-\right) \tag{5}$$

where $(\hat{\sigma}_\pm)$ and $\hat{\sigma}_z$ are Pauli operator while ω_0 is the energy difference between the atomic level. Since the model can describe a system of N two-level atom, therefore it would be interested to refer to the work by the authors of Ref. [27] where they analyzed the evolution of collective spontaneous emission from an ensemble of N identical two-level atoms

prepared by absorption of a single photon (termed Dicke state) superradiance. In the next section we introduce the solution of the wave function governed by (5) by employing the Heisenberg equations of motion and using the evolution operator to find the wave function of the system, from which we discuss the atomic inversion in Section 3. In Section 4 we examine the degree of entanglement. This is followed by the entropy squeezing and the variance squeezing in Sections 5.1 and 5.2. While we devote Section 6 to consider the correlation function while we give our conclusion in Section 7.

2 The Wave Function

Our main task in this section is to obtain the time-dependent wave function for the Hamiltonian (5). To do so we first introduce the operations of the operators $\hat{J}^2 = \hat{J}_z^2 + \frac{1}{2}\left(\hat{J}_-\hat{J}_+ + \hat{J}_+\hat{J}_-\right)$ and $\hat{J}_z$ on the state $|j,m\rangle$ which is the eigenstate of the operators $\hat{J}_\pm$ and $\hat{J}_z$ which satisfy the following relations

$$\begin{aligned}
\hat{j}^2|j,m\rangle &= j\,(j+1)\,|j,m\rangle, \qquad \hat{j}_z|j,m\rangle = m|j,m\rangle,\\
\hat{j}_+|j,m\rangle &= \sqrt{(j-m)\,(j+m+1)}|j;m+1\rangle,\\
\hat{j}_-|j,m\rangle\rangle &= \sqrt{(j+m)\,(j-m+1)}|j;m-1\rangle,
\end{aligned} \tag{6}$$

To obtain the constants of motion we use the Heisenberg equations of motion for the operator $\hat{O}$, namely $\frac{i}{\hbar}\left[\hat{H},\,\hat{O}\right]$, then we have

$$\begin{aligned}
i\,\dot{J}_z &= -\lambda\left(\hat{J}_-\hat{\sigma}_+ - \hat{J}_+\hat{\sigma}_-\right)\\
i\dot{\sigma}_z &= 2\lambda\left(\hat{J}_-\hat{\sigma}_+ - \hat{J}_+\hat{\sigma}_-\right),
\end{aligned} \tag{7}$$

from which we can deduce that the operator,

$$\hat{N} = \hat{J}_z + \frac{1}{2}\hat{\sigma}_z, \tag{8}$$

where $\hat{N}$ is a constant of motion.

Therefore, the Hamiltonian (5) can be cast in the following form

$$\hat{H}/\hbar = \hat{\Lambda} + \hat{C} \tag{9}$$

where the operators $\hat{\Lambda}$ and $\hat{C}$ are given by

$$\begin{aligned}
\hat{\Lambda} &= \omega\hat{N} + \chi\left(\hat{N}^2 + \frac{1}{4}\right),\\
\hat{C} &= \frac{\hat{\delta}}{2}\,\hat{\sigma}_z + \lambda\left(\hat{J}_-\hat{\sigma}_+ + \hat{J}_+\hat{\sigma}_-\right).
\end{aligned} \tag{10}$$

The quantity $\hat{\delta}$ is the detuning parameter defined by

$$\hat{\delta} = \left(\omega_0 - \omega - 2\chi\hat{N}\right). \tag{11}$$

It is interesting to point out that the existence of the Kerr parameter χ leads $\hat{\delta}$ to acquire the constant operator $\hat{N}$.

It is easy to show that the operators $\hat{\Lambda}$ and $\hat{C}$ commute, and hence each of them commute with the Hamiltonian $\hat{H}$. This means that the operators $\hat{\Lambda}$ and $\hat{C}$ are constants of motion.

The time evolution operator $\hat{U}(t)$ given by $\hat{U}(t) = \exp[-i\, t\hat{H}/\hbar]$, can be written in the form

$$U(t) = \exp[-i\hat{C}t] \times \exp\left[-i\hat{\Lambda}t\right] \tag{12}$$

The exponential operator has form

$$\exp[-i\hat{C}t] = \begin{bmatrix} \left(\cos\hat{\mu}_1 t - \frac{i\delta_1}{\hat{\mu}_1}\sin\hat{\mu}_1 t\right) & -i\lambda\frac{\sin\hat{\mu}_1 t}{\hat{\mu}_1}\hat{J}_- \\ -i\lambda\hat{J}_+\frac{\sin\hat{\mu}_1 t}{\hat{\mu}_1} & \left(\cos\hat{\mu}_2 t + \frac{i\delta_2}{\hat{\mu}_2}\sin\hat{\mu}_2 t\right) \end{bmatrix}, \tag{13}$$

where

$$\begin{aligned} \mu_l^2 &= \delta_l^2 + \nu_l, \quad l = 1, 2 \qquad \hat{\nu}_1 = \lambda^2\hat{J}_-\hat{J}_+, \qquad \hat{\nu}_2 = \lambda^2\hat{J}_+\hat{J}_- \\ \hat{\delta}_1 &= \omega_0 - \omega - 2\chi\left(\hat{J}_z + \frac{1}{2}\right) \\ \hat{\delta}_2 &= \omega_0 - \omega - 2\chi\left(\hat{J}_z - \frac{1}{2}\right) \end{aligned} \tag{14}$$

Note that the dependence of the detuning parameters on the operator $\hat{J}_z$ is due to the nonlinear dependence in the Hamiltonian.

Now let us define the atomic coherent state $|\theta, \phi\rangle$ which acquires both excited state $|e\rangle$ and ground state $|g\rangle$ for the two-level atoms in the following form

$$|\theta, \phi\rangle = \cos(\theta/2)|e\rangle + \sin(\theta/2)\exp(-i\phi)|g\rangle, \tag{15}$$

where θ is the coherence angle and ϕ is the relative phase of the two atomic levels. To reach the excited state we have to take $\theta \to 0$ while to make the wave function describes the particle in the ground state we have to let $\theta \to \pi$. If we assume that at the time $t = 0$ the system is in a pure state, then the wave function may take the form

$$|\psi(0)\rangle = |\theta, \phi\rangle \otimes |\alpha, \beta\rangle \tag{16}$$

where

$$|\alpha, \beta\rangle = \sum_{m=-j}^{m=j} Q(m, j)|j, m\rangle, \quad Q(m, j) = \left(\sin\frac{\alpha}{2}\right)^{j-m}\left(\cos\frac{\alpha}{2}\right)^{j+m} e^{i(j-m)\beta}\left[\binom{2j}{j-m}\right]^{\frac{1}{2}} \tag{17}$$

which is a coherent state of the su(2) group.

Therefore, if we drop the factor $\exp\left(-i\hat{\Lambda}t\right)$ which will produce a phase factor and use (13), after minor calculations the wave function for $t > 0$ takes the form

$$\begin{aligned} |\psi(t)\rangle &= \left\{\left(\cos\hat{\mu}_1 t - \frac{i\hat{\delta}_1}{\mu_1}\sin\hat{\mu}_1 t\right)\cos\frac{\theta}{2} - i\lambda\frac{\sin\hat{\mu}_1 t}{\mu_1}\hat{J}_-\right. \\ &\quad \left.\times\exp\{-i\phi\}\sin\frac{\theta}{2}\right\}|\alpha, \beta, e\rangle + \left\{\left(\cos\hat{\mu}_2 t + \frac{i\hat{\delta}_2}{\mu_2}\sin\hat{\mu}_2 t\right)\right. \\ &\quad \left.\times\exp\{-i\phi\}\sin\frac{\theta}{2} - i\lambda\frac{\sin\hat{\mu}_2 t}{\mu_2}\hat{J}_+\cos\frac{\theta}{2}\right\}|\alpha, \beta, g\rangle. \end{aligned} \tag{18}$$

Note that the authors of Ref. [28] managed to find the solution of the wave function beyond adiabatic approximation. Now we are in a position to write the reduced density matrix for the field subsystem which is given by $\hat{\rho}_f(t) = Tr_{atom}|\psi(t)\rangle\langle\psi(t)|$, such that

$$\hat{\rho}_f(t) = |D(t)\rangle\langle D(t)| + |T(t)\rangle\langle T(t)|, \tag{19}$$

where we define

$$|D(t)\rangle = \left\{\left(\cos\hat{\mu}_1 t - \frac{i\hat{\delta}_1}{\mu_1}\sin\hat{\mu}_1 t\right)\cos\frac{\theta}{2} - i\lambda\frac{\sin\hat{\mu}_1 t}{\mu_1}\hat{j}_-\exp\{-i\phi\}\sin\frac{\theta}{2}\right\}|\alpha,\beta\rangle, \tag{20}$$

and

$$|T(t)\rangle = \left\{\left(\cos\hat{\mu}_2 t + \frac{i\hat{\delta}_2}{\mu_2}\sin\hat{\mu}_2 t\right)\exp\{-i\phi\}\sin\frac{\theta}{2} - i\lambda\frac{\sin\hat{\mu}_2 t}{\mu_2}\hat{j}_+\cos\frac{\theta}{2}\right\}|\alpha,\beta\rangle. \tag{21}$$

By employing the reduced density operator given by (19) and using (20), (21), we can discuss some statistical properties of the present system. This will be done in the next sections.

3 Atomic Inversion

The atomic inversion describes the difference between the probability of finding the atom in its upper state $|e\rangle$ and lower states $|g\rangle$. The phenomenon of collapses and revivals represents one of the most important nonclassical phenomena in the field of quantum optics. The observation of this phenomenon occurs during the interaction between the subsystems within a cavity. Therefore to display the behavior of the atomic inversion we plot Fig. 1 for the function against the scaled time λt for different values of the involved parameters.

The atomic inversion is obtained as the expectation value of the operator $\hat{\sigma}_z$ thus one uses (20) and (21) to get

$$W(t) = \langle\hat{\sigma}_z(t)\rangle = \langle D(t)|D(t)\rangle - \langle T(t)|T(t)\rangle \tag{22}$$

For example we fixed the value of the parameters $\alpha = \pi/3$, $\beta = \pi/4$, $\phi = 0$ and $\theta = 0$. In Fig. 1a, for $\chi = 0$ and $j = 20$, we can see a short period of collapse which is followed by period of revival with oscillations around the *zero* value. Consequently several quiescent periods with successive several small periods of partial revivals are observed. An increase of the value of χ as $\chi = 0.75$, leads the function to show collapse period longer than the previous case. This is followed by a long period of revival that fluctuates around 0.1, see Fig. 1b. Also quiescent periods appear before interference takes over A shift upwards of the curve is displayed which means that more energy is stored in the atomic system. A period of collapse is seen for the case $\chi = 0$ and $j = 60$ after the onset of the interaction which is followed by interfering revival periods. see Fig. 1c. Superstructure phenomenon is observed by increasing the value of j while the fluctuations are around zero due to taking $\chi = 0$.

The function shows period of collapse after the onset of the interaction which is followed by a long period of revival and hence we can also see periods of interfering revivals and the function fluctuates around 0.1, for the case $\chi/\lambda = 0.75$ and $j = 60$, see Fig. 1d. Finally we would like to point out that, during the collapses periods there are interference between the patterns and the phenomenon of super structure appear. Furthermore increasing the value of

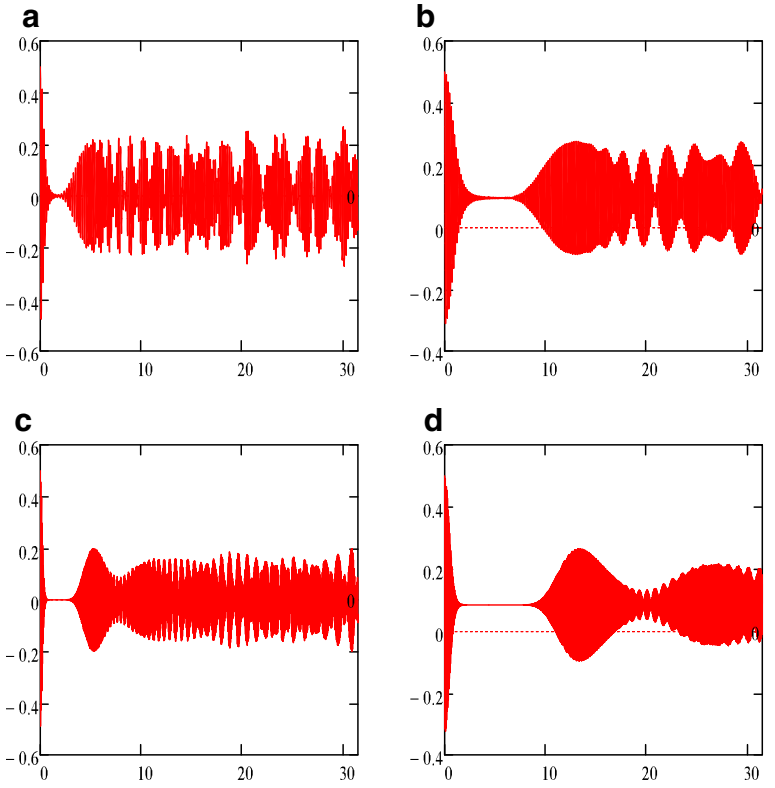

Fig. 1 The atomic inversion against the scaled time λt, with fixed parameters $\alpha = \frac{\pi}{3}$, $\beta = \frac{\pi}{4}$, $\phi = 0, \theta = 0$, where (**a**) $\chi = 0$, $j = 20$ (**b**)$\chi/\lambda = 0.75$, , $j = 20$ (**c**) $\chi = 0$, $j = 60$ (**d**) $\chi/\lambda = 0.75$, $j = 60$

χ/λ tends to shift the curve upwards which means that the energy tends to be stored in the atomic system.

4 Linear Entropy

We devote this section to discuss the degree of entanglement where we use the reduced entropy theory to study the dynamical coherence of state [29]. Quantum entropy is most commonly defined using the von Neumann [30] or Shannon entropy [31]. Meanwhile, it has shown that the initial entangled state can be deduced from the nonstationary autocorrelation function which in consistent with the present system [32]. To do so we use the purity as defined before [33–35]. This is an important physical quantity, related to both information content and to thermodynamic behavior which is defined by [36]

$$\zeta_F = \left[1 - \left(\langle\sigma_z\rangle^2 + \langle\sigma_x\rangle^2 + \langle\sigma_y\rangle^2\right)\right] \tag{23}$$

It should be noted that, when the state-vector description of each individual system of the ensemble is possible, a necessary and sufficient condition for the ensemble to be described in terms of a pure state is that $\zeta_F = 0$. However, for the case in which $\zeta_F < 1$, the system is in a statistical mixture state. We use the same data of the involved parameters as in the

previous case to plot Fig. 2. For $\chi = 0$ and $j = 20$ the function displays partial entanglement and also reaches the maximum entanglement at several periods of the time, see Fig. 2a. When the Kerr parameter coupler takes place, for example $\chi/\lambda = 0.75$ this leads to rapid fluctuations with interference between patterns where the superstructure phenomenon gets pronounced. On the other hand the function shows reduction in its maximum values which occurs few times, see Fig. 2b. Furthermore the function shows dense oscillations for $j = 60$ and $\chi = 0$ and its minimum value is decreased compared with the case of $j = 20$ and $\chi = 0$, in addition it shows a long period of maximum entanglement. In fact we observe that its minimum value is reduced below 0.2 during a period after onset of interaction showing partial entanglement compared with the other two cases, see Fig. 2c. Finally we realize that when $\chi/\lambda = 0.75$ and $j = 60$, the function shows increase in its minimum and decrease in its maximum and does not reach maximum entanglement during the considered period of time, with elongation of the periods, see Fig. 2d. Therefore the coupler tends to reduce entanglement and elongates the periods.

5 Squeezing

The squeezing phenomenon is one of the nonclassical phenomena in the field of quantum optics. There are different kinds of the squeezing that can be used to discuss the

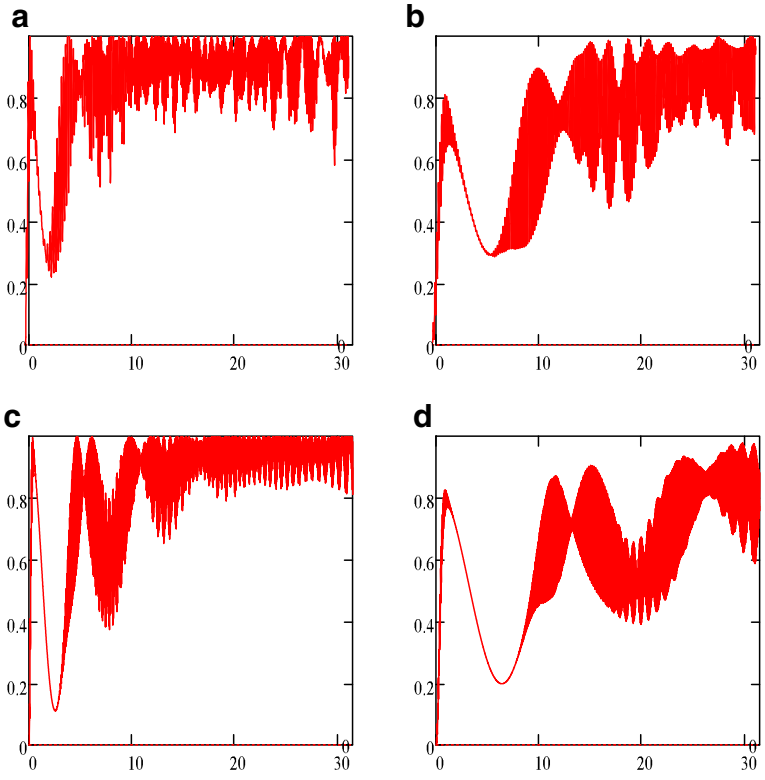

Fig. 2 The linear entropy against the scaled time λt, with fixed parameters $\alpha = \frac{\pi}{3}$, $\beta = \frac{\pi}{4}$, $\phi = 0, \theta = 0$, where (**a**) $\chi = 0$, $j = 20$ (**b**) $\chi/\lambda = 0.75$, $j = 20$ (**c**) $\chi = 0$, $j = 60$ (**d**) $\chi/\lambda = 0.75$, $j = 60$

negativity of the quadrature variances of the system. This depends on which Hamiltonian describes the system. For example, the normal and the principle squeezing are used for system that contains photon operators. Meanwhile the entropy squeezing and variance squeezing can be used for system that contains atoms. In fact it is possible to transfer the Einstein–Podolsky–Rosen-type continuous-variable entanglement from the squeezed light to the mechanical motion of the movable mirrors [37]. Note that stationary entanglement of the states of the movable mirrors as strong as that of the input squeezed light can be obtained for sufficiently large optomechanical cooperativity, achievable in currently available optomechanical systems.

5.1 Entropy Squeezing

In what follows we discuss the entropy and atomic variable squeezing. This is due to their importants in the field of quantum optics. For example it was shown that the optomechanical coupling can lead to squeezing of the nanomechanical motion, which can be inferred from the measurement of the squeezing of the transmitted microwave field, see for example [38] and references therein. The authors of this refrence investigated the squeezing properties of the transmitted microwave field in the presence of the nonlinearity induced by superconducting qubit (represented by the effective coupling) as well as the nonlinearity due to the optomechanical coupling. It is well known that the uncertainty relation of the information entropy can be used as a general criterion for the squeezing of a system. The information entropy of the operators $\hat{\sigma}_k$ for two-level atom is given by [39, 40]

$$H\langle\hat{\sigma}_k\rangle = -\frac{1}{2}\sum_{i=1}^{2}\left[1+(-1)^i\langle\hat{\sigma}_k\rangle\right]\ln\left[1+(-1)^i\langle\hat{\sigma}_k\rangle\right] \tag{24}$$

The uncertainty relations of the information entropy can be used as a general criterion for the squeezing in the entropy. Consequently the entropies of these operators satisfy the entropy uncertainty relation [41]

$$H(\sigma_x)+H(\sigma_y)+H(\sigma_z)\geq 2\ln 2. \tag{25}$$

Therefore, we have $0 \leq H(\sigma_k) \leq \ln 2$, provided we take $\delta H(\sigma_\alpha) \equiv \exp[H(\sigma_\alpha)]$, the entropy uncertainty relation becomes

$$\delta H(\sigma_x)\delta H(\sigma_y)\delta H(\sigma_z)\geq 4, \tag{26}$$

The fluctuations in the components σ_k of a qubit are said to be "squeezed in entropy" if the information entropy $H(\sigma_k)$ satisfies the condition

$$E_k = \delta H(\sigma_k) - \frac{2}{\sqrt{\delta H(\sigma_z)}} < 0, k \equiv x \ or \ y. \tag{27}$$

For this reason we plot Fig. 3 to examine the entropy squeezing where we have changed the value of $\alpha = 0.05\pi$ and $\chi/\lambda = 0.25$ and the rest of the data as in the previous cases. For example we consider $\chi = 0$ and $j = 20$ to plot Fig. 3a where the entropy squeezing occurs in both quadratures $E_x(t)$ (blue solid curve) and $E_y(t)$ (red dashed curve). Also it is noted that there is exchange between the quadratures. Irregular fluctuations are observed in both quadratures when we take $\chi/\lambda = 0.25$ in addition to reduction in the minimum value of the squeezing, see Fig. 3b. For $\chi = 0$ and $j = 60$, we can see exchange between the two quadratures, as well as regular fluctuations with some interference between the patterns. Furthermore the minimum value of the first quadrature $E_x(t)$ is decreased but there is an increase in its maximum values. Similar behavior is seen in the second quadrature $E_y(t)$,

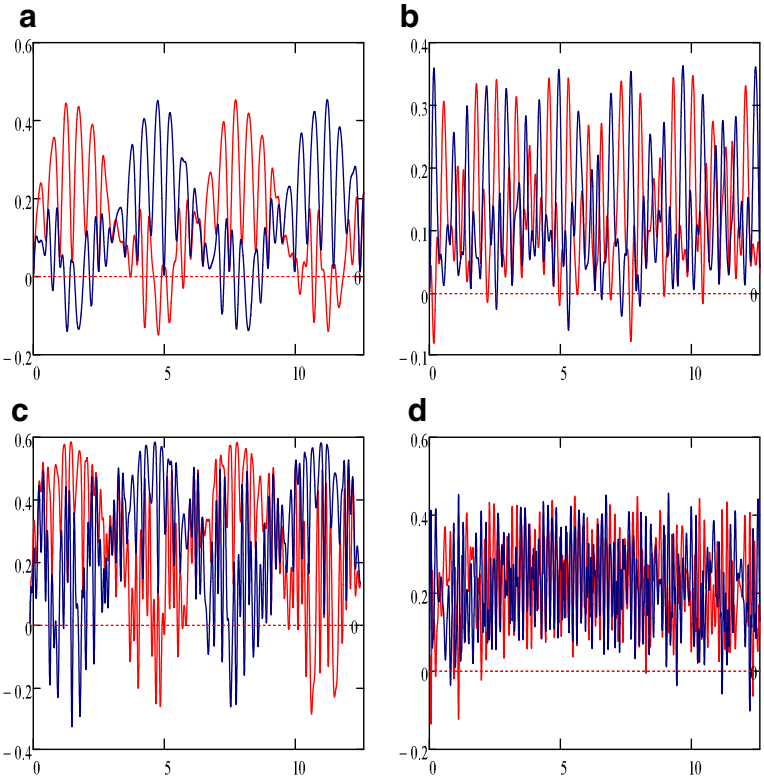

Fig. 3 The entropy squeezing against the scaled time λt, with fixed parameters $\alpha = 0.05\pi,\ \beta = \frac{\pi}{4},\ \phi = 0, \theta = 0$, where (**a**) $\chi = 0,\ j = 20$ (**b**) $\chi/\lambda = 0.25,\ j = 20$ (**c**) $\chi = 0,\ j = 60$ (**d**) $\chi/\lambda = 0.25, j = 60$

but the minimum value of the squeezing is greater than that of $E_x(t)$, see Fig. 3c. When we consider $\chi/\lambda = 0.25$ the quadratures squeezing reduces their minimum and consequently the amount of the squeezing. In the meantime more repaid fluctuations can be seen in both quadratures, see Fig. 3d. The effect of the coupler parameter is to deteriorate squeezing in the entropy.

5.2 Atomic Variable Squeezing

For the quantum mechanical system with two physical observables represented by the Hermitian operators $\hat{A}$ and $\hat{B}$ satisfying the commutation relation $[\hat{A}, \hat{B}] = i\hat{C}$, one can write the Heisenberg uncertainty relation in the form

$$\langle(\Delta\hat{A})^2\rangle\langle(\Delta\hat{B})^2\rangle \geq \frac{1}{4}|\langle\hat{C}\rangle|^2, \tag{28}$$

where $\langle(\Delta\hat{A})^2\rangle = (\langle\hat{A}^2\rangle - \langle\hat{A}\rangle^2)$. Consequently, the uncertainty relation for a two-level atom characterized by the Pauli operators $\hat{\sigma}_x$, $\hat{\sigma}_y$ and $\hat{\sigma}_z$, satisfying the commutation relation $\left[\hat{\sigma}_x, \hat{\sigma}_y\right] = 2i\hat{\sigma}_z$ can also be written as $\Delta\hat{\sigma}_x\Delta\hat{\sigma}_y \geq |\langle\hat{\sigma}_z\rangle|$.

Fluctuations in the component $\Delta\hat{\sigma}_\alpha$ of the atomic dipole is said to be squeezed if $V(\hat{\sigma}_\alpha)$ satisfies the condition

$$V(\hat{\sigma}_\alpha) = \left(\Delta\hat{\sigma}_\alpha - \sqrt{|\langle\hat{\sigma}_z\rangle|}\right) < 0, \quad \alpha = x \quad \text{or} \quad y. \tag{29}$$

In order to discuss the atomic variable squeezing, we plot Fig. 4 against the scaled time for different values of j and χ. For instance we examine the case in which $j = 20$ and $\chi = 0$, where we observe exchange between squeezing in quadrature variances $V_x(t)$ (blue solid curve) and $V_y(t)$ (red dashed curve) in addition to small amount of squeezing in both quadratures, see Fig. 4a. When we increase the value of $\chi/\lambda = 0.75$ we see rapid fluctuations in both quadrature variances with reduction in the squeezing amount, see Fig. 4b. More periods of the squeezing with decreasing in the quadratures minimum value when we consider $j = 60$ and $\chi = 0$, see Fig. 4c. Different shape is realized in the quadrature variances for $j = 60$ and $\chi = 0.75$, where the periods of the squeezing decreased in addition to rapid fluctuations with heavy interference between the patterns and the phenomenon of super-structure gets pronounced. The coupler seems to increase the oscillations of the curves of squeezing, but it leads to deteriorate squeezing.

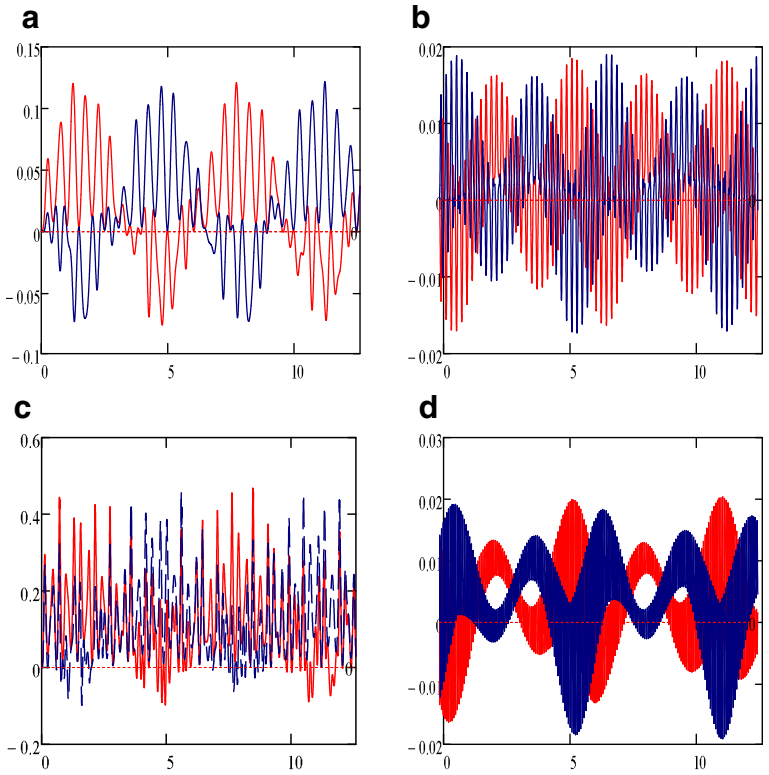

Fig. 4 The atomic variable squeezing against the scaled time λt, with fixed parameters $\alpha = 0.05\pi$, $\beta = \frac{\pi}{4}$, $\phi = 0, \theta = 0$, where (**a**) $\chi = 0, j = 20$ (**b**) $\chi/\lambda = 0.75, j = 20$ (**c**) $\chi = 0, j = 60$ (**d**) $\chi/\lambda = 0.75, j = 60$

6 Correlation Function

The examination of the correlation function leads to show whether the system produces classical or nonclassical behavior, or both of them. This function is called Glauber second order correlation function [42] and is defined for $Su\,(2)$ Lie algebra as follows

$$g^{(2)}(t) = \frac{\left\langle \hat{J}_+^2(t)\hat{J}_-^2(t)\right\rangle}{\langle \hat{J}_+(t)\hat{J}_-(t)\rangle^2} \tag{30}$$

The system produces sub-Poisonian (nonclassical) behavior if $g^{(2)}(t) < 1$, and it shows super-Poisonian if $g^{(2)}(t) > 1$. However, the system becomes Poisonian for $g^{(2)}(t) = 1$.

To examine the behavior of the function we plot Fig. 5 using the same data as in previous sections. For instance we consider the case in which $\chi = 0$ and $j = 20$, where the function displays sub-Poisoian as well as super-Poisonian. However the periods of the sub-Poisonian is longer than the super-Poisonian, in the meantime it shows fluctuations between the values 0.65 and just above 1.2, see Fig. 5a. When the Kerr coupler takes place, i.e. $\chi/\lambda = 0.75$ the function increases its fluctuations for long period of time, its minimum is just above 0.9, while its maximum is just above 1.1. In the meantime the amplitude of the function decreases as the time increases after it reaches its maximum, however the sub-Poisnian behavior washed out, see Fig. 5b. For the case $\chi = 0$ and $j = 60$ the nonclassical behavior

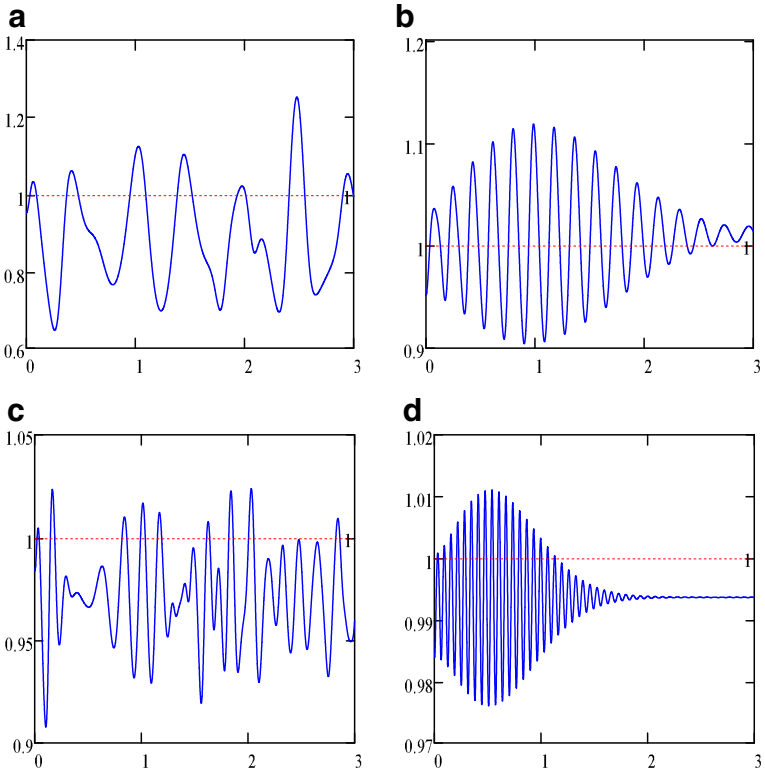

Fig. 5 The correlation function against the scaled time λt, with fixed parameters $\alpha = 0.05\pi$, $\beta = \frac{\pi}{4}$, $\phi = 0$, $\theta = 0$, where (**a**) $\chi = 0$, $j = 20$ (**b**) $\chi = 0.75$, $j = 20$ (**c**) $\chi = 0$, $j = 60$ (**d**) $\chi = 0.75$, $j = 60$

gets pronounced but lesser than before while the classical observed for short periods of the time, see Fig. 5c. Finally when we consider the Kerr coupler $\chi/\lambda = 0.75$ the function starts to increase its amplitude after the onset of the interaction until to reach its maximum and then we can observe both nonclassical and classical behavior. Consequently it starts to decrease its extrema as the time increases and then it shows nonclassical behavior for long period of the time, see Fig. 5d. Thus we may conclude that increasing the parameter χ and J amounts to get nonclassical behavior for longer time.

7 Conclusion

In the previous sections of the present communication we have considered the problem of the interaction between a two-level atom and the co-directional Kerr nonlinear coupler in terms of su(2) Lie algebra. The wave function is obtained via the evolution operator and consequently we managed to construct the time-dependent density operator. We employed this result to discuss the atomic inversion for certain values of χ and the quantum number j where we found an increasing in the value of both parameter leads to increase the revival period and storing of the energy in the atomic system. In the meantime the maximum entanglement is found when $\chi = 0$,while the linear entropy in general is sensitive to the variation in χ and j. We also examined the entropy and atomic variable squeezing where we observe that there is exchange between squeezing in the quadrature. Moreover an increase in the value of the quantum number leads to more fluctuations and consequently we observe superstructure phenomenon, but an increase in the coupler parameter χ tends to decrease the amounts of squeezing. For the correlation function the nonclassical phenomenon is pronounced for all the cases we have examined, and increasing χ leads to prolong the periods of non classicality.

Acknowledgments M.S.Abdalla extends his appreciation to the Deanship of Scientific Research at KSU for funding the work through the research group project No.PRG/1436/22.

References

1. Jensen, S.M.: IEEE J. Quant. Electron. QE **18**, 1580 (1982)
2. Ekert, A., Jozsa, R.: Rev. Mod. Phys. **68**, 733 (1996)
3. Lo, H.-K., Popescu, S., Spiller, T.: Introduction to quantum computation and information. World Scientific, Singapore (1998)
4. Begie, A., Braun, D., Tregenna, B., Knight, P.L.: Phys. Rev. Lett. **85**, 1762 (2000)
5. Assanto, G., Stegeman, G.I., Sheik-Bahae, M., Van Stryland, E.W.: Appl. Phys. Lett. **62**, 1323 (1993)
6. Karpierz, M., Wolinski, T., Swillo, M.: Molec. Cryst. Liq. Cryst. **282**, 365 (1996)
7. Chefles, A., Barnett, S.M.: J. Mod. Opt. **43**, 709 (1996)
8. Townsend, P.D., Baker, G.L., Shelburne, J. L. III., Etemad, S.: Proc. SPIE **1147**, 256 (1989)
9. Fazio, E., Sibilia, C., Senesi, F., Bertolotti, M.: Opt. Commun. **127**, 62 (1996)
10. Brooks, D., Ruschin, S., Scarlat, D.: IEEE J. Select. Top. Quant. Electr. **2**, 210 (1996)
11. Luff, B.J., Harris, R.D., Wilkinson, J.S., Wilson, R., Schiffrin, D.J.: Opt. Lett. **21**, 618 (1996)

12. Guo, A., Henry, M., Salamo, G.J., Segev, M., Wood, G.L.: Opt. Lett. **26**, 1274 (2001)
13. Wang, Q., He, S.: IEEE J. Select. Top. Quant. Electr. **8**, 1233 (2002)
14. Zhou, B., Xu, C.-Q., Chen, B.: J. Opt. Soc. Am. B **20**, 846 (2003)
15. Finlayson, N., Banyai, W.C., Wright, E.M., Seaton, C.T., Stegeman, G.I., Cullen, T.J., Ironside, C.N.: Appl. Phys. Lett. **53**, 1144 (1988)
16. Soldano, L.B., Pennings, E.C.M.: J. Lightwave Technol. **13**, 615 (1995)
17. Tricca, D., Sibilia, C., Severini, S., Bertolotti, M., Scalora, M., Bowden, C.M., Sakora, K.: J. Opt. Soc. Am. B **21**, 671 (2004)
18. Peřina, J., Peřina, Jr., J.: J. Mod. Opt. **43**, 1951 (1996)
19. Abdalla, M.S., El-Orany, F.A.A., Peřina, J.: J. Phys. A: Math. Gen. **32**, 3457 (1999)
20. Abdalla, M.S., El-Orany, F.A.A., Peřina, J.: J. Mod. Opt. **47**, 1055 (2000)
21. Peřina, J., Peřrina, J.r., J.: Quant. Semiclass. Opt. **7**, 541 (1995)
22. Peřina, J.: J. Mod. Opt. **42**, 1517 (1996)
23. El-Orany, F.A.A., Peřina, J., Abdalla, M.S.: Quant. Semiclass. Opt. **3**, 67 (2001)
24. El-Orany, F.A.A., Peřina, J., Abdalla, M.S.: Phys. Scr. **63**, 128 (2001)
25. El-Orany, F.A.A., Peřina, J., Abdalla, M.S.: Inter. J. Mod. Phys. B **15**, 2125 (2001)
26. Hořak, R., Bertolotti, M., Sibilia, C., Peřina, J.: J. Opt. Soc. Am. B **6**, 199 (1989)
27. Setea, E., Svidzinsky, A.A., Eleuch, H., Yanga, Z., Nevelsa, R.D., Scully, M.O.: J. Mod. Opt. **57**, 1311 (2010)
28. Eleuch, H., Rostovtsev, Y.V., Scully, M.O.: EPL **89**, 50004 (2010)
29. Abdalla, M.S., Khalil, E.M., Obada, A.S.-F.: Phys. A **466**, 4456 (2017)
30. Knight, P.L., Radamore, P.M.: Phys. Lett. A **90**, 342 (1982)
31. Yoo, H.I., Eberly, J.H.: Phys. Rep. **118**, 239 (1981)
32. Eleuch, H.: Inter.J. Mod. Phys. B **24**, 5653 (2010)
33. Zurek, W.H., Habib, S., Paz, J.P.: Phys. Rev. Lett. **70**, 1187 (1993)
34. Kim, J.I., Nemes, M.C., De Toledo Piza, A.F.R., Borges, H.E.: Phys. Rev. Lett. **77**, 207 (1996)
35. Isar, A., Sandulescu, A., Scheid, W.: Phys. Rev. E **60**, 6371 (1999)
36. El-Orany, F.A.A., Abdalla, M.S.: J. Phys. A. Math. Theor. **44**, 035302 (2011)
37. Sete, E.A., Eleuch, H., Raymond Ooi, C.H.: J. Opt. Soc. Am. B **31**, 2821 (2014)
38. Sete, E.A., Eleuch, H.: Phys. Rev. A **89**, 013841 (2014)
39. Shannon, C.C.: Bell. Syst. Tech. J **27**, 379 (1948)
40. Fang, M.F., Zhon, P., Swain, S.: J. Mod. Opt. **47**, 1093 (2000)
41. Bertet, P., Auffeves, A., Maioli, P., Osnaghi, S., Meunier, T., Brune, M., Raimond, J.M., Haroche, S.: Phys. Rev. Lett. **89**, 2200402-1 (2002)
42. Garry, C.C., Knight, P.: Introductory quantum optics, Cambridge University press. Cambridge